Low-Complexity Integrated Super-Resolution Sensing and Communication with Signal Decimation and Ambiguity Removal

DAI Qianglong[1], ZHOU Zhiwen[1], XIAO Zhiqiang[1,2], ZENG Yong[1,2], YANG Fei[3], CHEN Yan[3]

(1. National Mobile Communications Research Laboratory, Southeast University, Nanjing 210096, China;
2. Purple Mountain Laboratories, Nanjing 211111, China;
3. Wireless Technology Lab., 2012 Lab, Shanghai Huawei Technologies Co., Ltd, Shanghai 201206, China)

DOI: 10.12142/ZTECOM.202403007

https://kns.cnki.net/kcms/detail/34.1294.TN.20240812.1649.002.html, published online August 13, 2024

Manuscript received: 2024-07-30

Abstract: Integrated sensing and communication (ISAC) is one of the main usage scenarios for 6G wireless networks. To most efficiently utilize the limited wireless resources, integrated super-resolution sensing and communication (ISSAC) has been recently proposed to significantly improve sensing performance with super-resolution algorithms for ISAC systems, such as the Multiple Signal Classification (MUSIC) algorithm. However, traditional super-resolution sensing algorithms suffer from prohibitive computational complexity of orthogonal-frequency division multiplexing (OFDM) systems due to the large dimensions of the signals in the subcarrier and symbol domains. To address such issues, we propose a novel two-stage approach to reduce the computational complexity for super-resolution range estimation significantly. The key idea of the proposed scheme is to first uniformly decimate signals in the subcarrier domain so that the computational complexity is significantly reduced without missing any target in the range domain. However, the decimation operation may result in range ambiguity due to pseudo peaks, which is addressed by the second stage where the total collocated subcarrier data are used to verify the detected peaks. Compared with traditional MUSIC algorithms, the proposed scheme reduces computational complexity by two orders of magnitude, while maintaining the range resolution and unambiguity. Simulation results verify the effectiveness of the proposed scheme.

Keywords: ISSAC; sparse decimation; range ambiguity; two-stage approach

Citation (Format 1): DAI Q L, ZHOU Z W, XIAO Z Q, et al. Low-complexity integrated super-resolution sensing and communication with signal decimation and ambiguity removal [J]. ZTE Communications, 2024, 22(3): 48–55. DOI: 10.12142/ZTECOM.202403007

Citation (Format 2): Q. L. Dai, Z. W. Zhou, Z. Q. Xiao, et al., "Low-complexity integrated super-resolution sensing and communication with signal decimation and ambiguity removal," *ZTE Communications*, vol. 22, no. 3, pp. 48–55, Sept. 2024. doi: 10.12142/ZTECOM.202403007.

1 Introduction

Integrated sensing and communication (ISAC) has been identified as one of the key usage scenarios of the 6G communication systems[1]. However, due to the limited available wireless resources, the resolution of the classical inverse discrete Fourier transform/discrete Fourier transform (IDFT/DFT) based methods for sensing usually leads to poor performance[2]. To address such issues, integrated super-resolution sensing and communication (ISSAC) has been recently proposed to maximize the utilization of wireless resources and significantly enhance the sensing performance of ISAC systems[3]. Specifically, the ISSAC system exploits super-resolution algorithms for radar signal processing to achieve super-resolution parameter estimation, such as the angle-of-arrival (AoA), propagation delay, and the Doppler frequency shift of the targets.

On the other hand, orthogonal frequency division multiplexing (OFDM) is a dominate waveform in the 4G and 5G mobile communication systems, and it is expected to continue to play an important role in 6G. Consequently, besides dedicated waveform designs[4], extensive works on ISAC are still based on OFDM systems[2–3, 5–7]. For OFDM waveforms, the delay and Doppler estimation can be converted to spectral estimation problems due to the sum-of-complex-exponential structure of its channel matrix[7]. Various methods are proposed for OFDM-based sensing, such as the IDFT/DFT-based and subspace-based methods. The IDFT/DFT-based methods such as the periodogram algorithm[2] can be implemented easily but their resolution is limited by the wireless resources available for sensing, while the subspace-based methods, such as Mul-

This work was supported by the National Natural Science Foundation of China under Grant No. 62071114.

tiple Signal Classification (MUSIC)[8] and Estimation of Signal Parameters via Rotational Invariance Techniques (ESPRIT)[9], can achieve super-resolution but suffer from high computational complexity. Furthermore, compared with multiple-input multiple-output (MIMO) array signals for AoA estimation, the dimensions of OFDM signals in the subcarrier and symbol domains are extremely large. For example, when the number of antennas in an array reaches 128 or 512, it is called a massive array or an extremely large-scale array (XL-Array), but it is common for OFDM signals to have more than 512 subcarriers. Therefore, parameter estimation for OFDM waveforms suffers from prohibitive computational complexity if conventional super-resolution methods are directly applied. Extensive efforts have been devoted to reducing the complexity of such methods, like the ROOT-MUSIC[10–11] algorithm which replaces the spectrum search in MUSIC with polynomial rooting, or the Propagator Method (PM)[12–13] that replaces the eigenvalue decomposition by constructing a propagator. However, existing methods for complexity reduction are often tailored to specific algorithms, and thus their application scenarios are limited. Moreover, as these methods still struggle to address the high data dimension problem of OFDM signals, their complexity of delay and Doppler estimation remains high[14–15]. Thus, how to reduce the computational complexity for ISSAC is still an important problem not fully solved yet.

To address the above issues, we propose a novel and universal complexity reduction method for ISSAC systems. The key idea of the proposed method is to first reduce the data dimensions of OFDM signals through uniform and sparse decimation of the signals in the subcarrier domain, which significantly reduces the computational complexity without missing any sensing target. However, the decimation operation involves sparse signal resampling, which causes range ambiguity due to pseudo peaks. Then, a second stage is conducted to remove any ambiguity by checking all potential points individually using the total collocated subcarrier data. Due to the periodicity of the outputs of both IDFT/DFT-based and subspace-based methods[6], all the targets can be estimated using only a small subset of subcarriers, although range ambiguity may occur. Thus, we can first select a subset of the equidistance sparse subcarriers to reduce the data dimension, and then validate the estimated results using all the available subcarriers to remove any ambiguity. By utilizing the equidistance sparse data with lower subcarrier domain dimension in the first stage, the proposed method can achieve low-complexity range estimation with resolution equivalent to utilizing all the available data. Moreover, the proposed method is not only applicable to traditional super-resolution algorithms but also further reduces the complexity of existing low-complexity algorithms, e. g., PM-MUSIC and ROOT-MUSIC. Complexity analysis and simulation analysis are performed to verify the effectiveness of the proposed scheme. Numerical results demonstrate that the complexity of the proposed scheme is two orders of magnitude lower than the traditional MUSIC algorithm in minimal sensing performance degradation.

2 System Model

As shown in Fig. 1, we consider a mono-static OFDM-based ISSAC system, where a base station (BS) serves multiple communication user equipment (UE), and simultaneously senses multiple targets via the echoes of its transmitted signals. Note that the radar cross sections (RCSs) of communication UE are much smaller than those of the sensing targets, whose echoes are relatively small and can be neglected. The BS is equipped with M_t transmit antennas and a single radar receiving antenna. As we mainly focus on the range-Doppler sensing, analog beamforming is considered for the BS.

The BS transmits OFDM signals with N subcarriers and M OFDM symbols. The subcarrier spacing and the OFDM symbol duration with the cyclic prefix (CP) are denoted by Δf and T_s. The OFDM symbol duration without CP is $T = 1/\Delta f$, the duration of CP is $T_{cp} = T_s - T$, and the system bandwidth is $B = N\Delta f$. Therefore, the time-domain sequence of the m-th OFDM symbol transmitted by the BS before beamforming is

$$x_m[q] = \frac{1}{\sqrt{N}} \sum_{n=0}^{N-1} b_{n,m} e^{j2\pi nq/N}, \quad (1)$$

where $q = 0,1,\cdots,N-1$, and $b_{n,m}$ denotes the transmitted data on the n-th subcarrier of the m-th OFDM symbol.

Assuming that there are K targets for sensing. The range and the radial velocity of the k-th target are denoted by R_k and v_k, where $k = 1,2,\cdots,K$. Then, the delay and the Doppler frequency shift of the k-th target are $\tau_k = 2R_k/c = n_k\frac{1}{B}$ and $f_{dk} = 2f_cv_k/c$, where c denotes the signal propagation speed and f_c is the carrier frequency. To avoid inter-symbol interference (ISI), the maximum delay of the targets is assumed to be smaller than the CP duration. Moreover, the subcarrier spacing is assumed to be at least one order of magnitude larger than the largest Doppler frequency shift[7]. Note that mono-static ISAC systems necessitate full-duplex operation of the transmitter

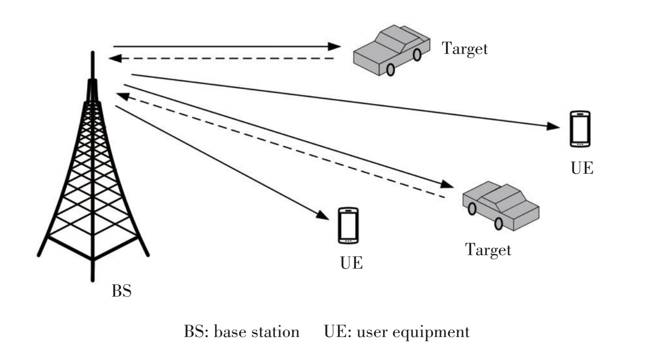

▲ **Figure 1. An illustration of the mono-static integrated super-resolution sensing and communication (ISSAC) system** and the radar receiver, making them vulnerable to self-interference (SI) due to imperfect isolation. Various methods have been proposed to address this issue, such as a combination of analog and digital cancellers[4]. After SI cancellation and CP removal, the time-domain sequence of the m-th received OFDM symbol is

$$y_m[q] = \sum_{k=1}^{K} \gamma_k x_m[q - n_k] e^{j2\pi m T_s f_{dk}} + \omega_m[q] = \sum_{k=1}^{K} \sum_{n=0}^{N-1} \gamma_k b_{n,m} e^{j2\pi\left(\frac{nq}{N} - n\Delta f \tau_k + mT_s f_{dk}\right)} + \omega_m[q], \quad (2)$$

where $\gamma_k = \frac{1}{\sqrt{N}} \boldsymbol{a}^H(\theta_k) \boldsymbol{w} \tilde{\gamma}_k$, $\boldsymbol{w} \in \mathbb{C}^{M_t \times 1}$ represents the transmit beamforming vector, $\boldsymbol{a}(\theta_k) \in \mathbb{C}^{M_t \times 1}$ and $\tilde{\gamma}_k$ denotes the array steering vector with angle of departure (AoD) θ_k and the complex reflection coefficient of the k-th target, and $\omega_m[q]$ is the corresponding additive white Gaussian noise (AWGN) plus the residual SI.

Then, $y_m[q]$ can be rearranged into a matrix $\boldsymbol{Y} \in \mathbb{C}^{N \times M}$ via DFT, and the (n,m)-th element of $\boldsymbol{Y}$ is

$$\boldsymbol{Y}(n,m) = \frac{1}{N} \sum_{q=0}^{N-1} y_m[q] e^{-\frac{j2\pi nq}{N}} = b_{n,m} \sum_{k=1}^{K} \gamma_k e^{-j2\pi n \Delta f \tau_k} e^{j2\pi m T_s f_{dk}} + \bar{\omega}_{n,m}, \quad (3)$$

where $\bar{\omega}_{n,m}$ is the resulting noise.

Since the transmitted data $b_{n,m}$ is known by the BS, it can be removed via element-wise division. By doing so, the data matrix $\tilde{\boldsymbol{Y}}(n,m) \in \mathbb{C}^{N \times M}$ for radar processing is

$$\tilde{\boldsymbol{Y}}(n,m) = \frac{\boldsymbol{Y}(n,m)}{b_{n,m}} = \sum_{k=1}^{K} \gamma_k e^{-j2\pi n \Delta f \tau_k} e^{j2\pi m T_s f_{dk}} + \bar{\omega}'_{n,m} \in \mathbb{C}^{N \times M}, \quad (4)$$

where $\bar{\omega}'_{n,m} = \frac{\bar{\omega}_{n,m}}{b_{n,m}}$. Therefore, the amplitude γ_k, the propagation delay τ_k, and the Doppler f_{dk} can be estimated with various estimation algorithms by utilizing the data matrix $\tilde{\boldsymbol{Y}}$.

Due to the large dimensions of the data matrix $\tilde{\boldsymbol{Y}}$, the computational complexity for parameter estimation is significantly high, especially for super-resolution algorithms like MUSIC. However, by exploiting the periodicity of the outputs of both IDFT/DFT-based and subspace-based methods, all the targets in the range domain can be estimated through sparse data in lower dimensions, although ambiguity may occur. This motivates us to reduce the computational complexity for parameter estimation by decimation, if the ambiguity can be removed. In the following section, we uniformly decimate the subcarrier domain data of the data matrix $\tilde{\boldsymbol{Y}}$ in Eq. (4) to reduce data dimension, and then exploit the range periodogram of decimated sparse data to analyze the relationship among the range resolution, the maximum unambiguous range and the decimation interval.

3 Ambiguity and Resolution Analysis

Since signal processing methods for range and Doppler estimations are similar, in the following, we focus on range estimation and assume all the targets are stationary, while the proposed method and analysis results can be directly applied to the Doppler counterparts. By uniformly decimating the subcarrier domain data of the data matrix $\tilde{\boldsymbol{Y}}$ in Eq. (4) with a step size of η, the decimated sparse data matrix can be expressed as

$$\tilde{\boldsymbol{Y}}^{\mathrm{sp}}(n^{\mathrm{sp}},m) = \tilde{\boldsymbol{Y}}(n^{\mathrm{sp}}\eta,m) = \sum_{k=1}^{K} \gamma_k e^{-j2\pi n^{\mathrm{sp}} \eta \Delta f \tau_k} + \bar{\omega}'_{n^{\mathrm{sp}}\eta,m}, \quad (5)$$

where $n^{\mathrm{sp}} = 0,1,\cdots,N^{\mathrm{sp}} - 1$, and $N^{\mathrm{sp}} = \left\lfloor \frac{N}{\eta} \right\rfloor$ denotes the number of subcarriers in the decimated sparse data.

Then, the IDFT is applied to each column of $\tilde{\boldsymbol{Y}}^{\mathrm{sp}}$, and the periodogram can be obtained by

$$\boldsymbol{F}(\tau;\eta) = \left| \frac{1}{M} \sum_{m=0}^{M-1} \frac{1}{N^{\mathrm{sp}}} \sum_{n^{\mathrm{sp}}=0}^{N^{\mathrm{sp}}-1} \tilde{\boldsymbol{Y}}^{\mathrm{sp}}(n^{\mathrm{sp}},m) e^{j2\pi n^{\mathrm{sp}} \eta \Delta f \tau} \right|^2. \quad (6)$$

The peaks of $\boldsymbol{F}(\tau;\eta)$ correspond to the ranges of targets, where $\tau = \frac{2R}{c}$ denotes the observation delay, and R denotes the observation range. When $\eta = 1$, the ranges of targets are estimated with the total collected data, while for $\eta > 1$, they are obtained with the decimated sparse data.

By ignoring the noise and substituting Eq. (5) into Eq. (6), the periodogram of decimated sparse data for range sensing can be obtained by

$$\boldsymbol{F}(\Delta\tau_k;\eta) = \left| \sum_{k=1}^{K} \gamma_k e^{-j\pi(N^{\mathrm{sp}}-1)\eta\Delta f \Delta\tau_k} \frac{\sin(\pi N \Delta f \Delta\tau_k)}{N^{\mathrm{sp}} \sin(\pi\eta\Delta f \Delta\tau_k)} \right|^2, \quad (7)$$

where $\Delta\tau_k = \frac{2\Delta_k}{c}$ denotes the delay difference, $\Delta_k = R - R_k \in [-d_{\mathrm{unamb}}, d_{\mathrm{unamb}}]$ denotes the range difference between the observation range R and the target range R_k, and $d_{\mathrm{unamb}} = \frac{c}{2\Delta f}$ denotes the maximum unambiguous range of OFDM radar with the subcarrier spacing Δf. It is observed from Eq. (7) that the range sensing for arbitrary target k is critically dependent on the function $G_\eta(\Delta_k) = \left| \frac{\sin(2\pi N \Delta f \Delta_k / c)}{N^{\mathrm{sp}} \sin(2\pi\eta\Delta f \Delta_k / c)} \right|^2$, which has the following properties.

Main lobe: Let $2\pi N\Delta f\Delta/c = \pm\pi$ or $\Delta = \pm\frac{c}{2N\Delta f}$, $G_\eta(\Delta) = 0$. Then the null-to-null width of the main lobe can be obtained as

$$\mathrm{BW} = \frac{c}{N\Delta f}. \tag{8}$$

Typically, the range resolution can be defined as a half of the main lobe width. Therefore, the range resolution of decimated sparse data is:

$$\Delta_r^{\mathrm{res}} = \frac{1}{2}\mathrm{BW} = \frac{c}{2N\Delta f} = \frac{c}{2B}. \tag{9}$$

Grating lobe: When $\eta > 1$, grating lobes with the same amplitude and width as the main lobe exist, and the locations of the grating lobes can be obtained by letting $\frac{2\pi\eta\Delta f\Delta}{c} = n\pi, n = \pm1,\pm2,\cdots,\pm\eta$. Then the n-th grating lobe is located at:

$$\Delta = \frac{nc}{2\eta\Delta f}, n = \pm1,\pm2,\cdots,\pm\eta. \tag{10}$$

The grating lobes reflect the periodicity of the periodogram, which will cause range ambiguity. The maximum unambiguous range achieved utilizing the decimated sparse data is the grating lobe interval $d_{\mathrm{unamb}}^{\mathrm{sp}} = \frac{c}{2\eta\Delta f}$.

For $N = 128$ and $\Delta f = 120$ kHz, Figs. 2(a) and 2(b) illustrate the range periodograms for collocated subcarrier data and decimated sparse data. It is observed that the decimated sparse data can achieve the same range resolution as the total collocated subcarrier data, while the maximum unambiguous range reduces inversely proportional to the decimation interval η. Similarly, when the decimated sparse data are applied in super-resolution algorithms, the range ambiguity exists and the range resolution remains. Moreover, the computational complexity of super-resolution algorithms is significantly high, especially for OFDM signals with high data dimensions. Therefore, it is necessary to propose low-complexity schemes utilizing lower-dimension decimated sparse data and periodic extension, while maintaining high range resolution. In the following section, we propose a two-stage scheme, which combines the advantages of collocated subcarrier data and decimated sparse data, to achieve low-complexity and unambiguous range sensing.

4 Range Sensing

4.1 Proposed Two-Stage Scheme

The two-stage scheme is shown in Fig. 3. In the first stage, we uniformly and sparsely decimate the subcarrier domain data from the matrix $\tilde{\boldsymbol{Y}}$ in Eq. (4) with decimation interval η. Thus, the range resolution and maximum unambiguous range of the decimated sparse data are $\Delta_r^{\mathrm{res,sp}} = \frac{c}{2B}$ and $d_{\mathrm{unamb}}^{\mathrm{sp}} = \frac{c}{2\eta\Delta f}$, respectively. By utilizing the decimated sparse data, all the possible ranges with ambiguity can be estimated. In the second stage, the range resolution and maximum unambiguous range of the total collocated data are $\Delta_r^{\mathrm{res}} = \frac{c}{2B}$ and $d_{\mathrm{unamb}} = \frac{c}{2\Delta f}$, and thus the range ambiguity can be removed by exploiting the collocated subcarrier data to check each range estima-

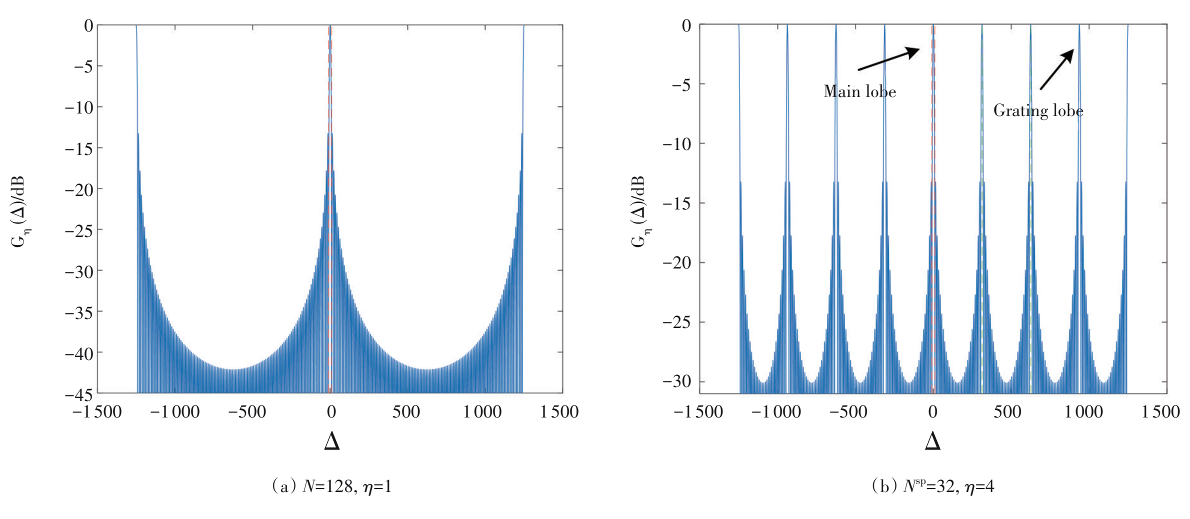

▲**Figure 2. Range periodograms of: (a) Collocated subcarrier data with the number of subcarriers N = 128 and (b) Decimated sparse data with decimation interval η = 4**

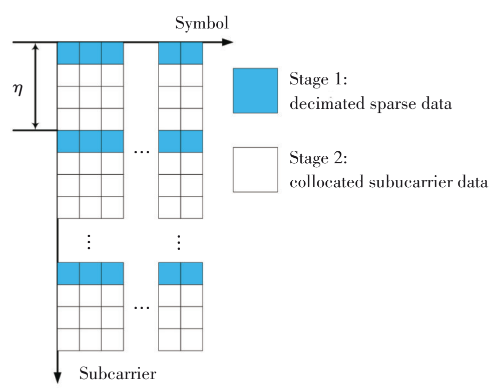

▲Figure 3. Illustration of the two-stage scheme

tion obtained in the first stage individually. Therefore, the two-stage scheme can achieve range resolution equivalent to utilizing the total collocated data in Eq. (4) without range ambiguity, while the computational complexity is much lower.

4.2 Proposed Two-Stage Algorithm

In this subsection, a novel two-stage algorithm based on MUSIC is proposed. To eliminate high correlation between echo signals of the targets, modified spatial smoothing preprocessing (MSSP)[16] is performed in the subcarrier domain of the data matrix $\tilde{\boldsymbol{Y}}$. Specifically, the smoothing window size is $N_L = \rho N$, $\rho = 0.5$, and the number of submatrices is $N_{\text{sub}} = N - N_L + 1$. Thus, the data matrix $\hat{\boldsymbol{Y}} \in \mathbb{C}^{N_L \times N_{\text{sub}} M}$ after MSSP can be obtained by:

$$\hat{\boldsymbol{Y}} = \begin{bmatrix} \tilde{\boldsymbol{y}}_1 & \cdots & \tilde{\boldsymbol{y}}_{N_{\text{sub}}} \\ \vdots & \ddots & \vdots \\ \tilde{\boldsymbol{y}}_{N_L} & \cdots & \tilde{\boldsymbol{y}}_{N_{\text{sub}} + N_L} \end{bmatrix}. \tag{11}$$

Then, the signal and noise subspaces can be obtained via eigenvalue decomposition (EVD) of the covariance matrix of the data matrix $\hat{\boldsymbol{Y}}$, which is expressed as:

$$\boldsymbol{R}_{\hat{Y}} = \frac{1}{N_{\text{sub}} M} \hat{\boldsymbol{Y}} \hat{\boldsymbol{Y}}^H = \boldsymbol{E}_s \boldsymbol{\Lambda}_s \boldsymbol{E}_s^H + \boldsymbol{E}_n \boldsymbol{\Lambda}_n \boldsymbol{E}_n^H, \tag{12}$$

where $\boldsymbol{\Lambda}_s$ denotes the diagonal matrix composed of the largest K eigenvalues, and $\boldsymbol{E}_s$ and $\boldsymbol{E}_n$ denote the signal subspace and noise subspace. Thus, the MUSIC spectrum for range estimation can be expressed as:

$$P_{\text{MUSIC}}(R) = \frac{1}{\boldsymbol{a}_r^H \boldsymbol{E}_n \boldsymbol{E}_n^H \boldsymbol{a}_r}, \tag{13}$$

where $\boldsymbol{a}_r = \left[1, e^{-j2\pi\Delta f \tau}, \cdots, e^{-j2\pi(N_L - 1)\Delta f \tau}\right]^{\text{T}}$, $\tau = \frac{2R}{c}$ denotes the steering vector in delay dimension, R denotes the observation range, and c denotes the wave propagation speed. The peaks of the MUSIC spectrum correspond to the ranges of the targets. The proposed two-stage algorithm works as follows. In the first stage, the possible ranges of the targets are obtained by first utilizing the MUSIC algorithm on the decimated matrix $\tilde{\boldsymbol{Y}}^{\text{sp}}$ and then periodically extending the peaks with interval $d^{\text{sp}}_{\text{unamb}}$. In the second stage, the MUSIC spectrum of collocated subcarrier data matrix $\tilde{\boldsymbol{Y}}$ is exploited to remove the range ambiguity, where the spectral values remain large at the true peaks and sharply decrease at the pseudo peaks. The detailed steps of the proposed algorithm are shown in Algorithm 1.

Algorithm 1. MUSIC based low-complexity two-stage algorithm

Inputs: total collocated subcarrier data matrix $\tilde{\boldsymbol{Y}}$;
the decimation interval η.
Outputs: estimated range $\hat{\boldsymbol{r}}$.
//Stage 1. Sparse estimation
1. $\tilde{\boldsymbol{Y}}^{sp} = \tilde{\boldsymbol{Y}}(1{:}\eta{:}N,:)$;
2. $N_L^{\text{sp}} = \rho N^{\text{sp}}$, $N_{\text{sub}}^{\text{sp}} = N^{\text{sp}} - N_L^{\text{sp}} + 1$;
3. Obtain sparse data matrix after MSSP $\hat{\boldsymbol{Y}}^{\text{sp}}$;
4. $\boldsymbol{R}_{\hat{Y}^{\text{sp}}} = \frac{1}{N_{\text{sub}}^{\text{sp}} M} \hat{\boldsymbol{Y}}^{\text{sp}} \hat{\boldsymbol{Y}}^{\text{sp}^H}$;
5. $\boldsymbol{R}_{\hat{Y}^{\text{sp}}} = \boldsymbol{E}_s^{\text{sp}} \boldsymbol{\Lambda}_s^{\text{sp}} \boldsymbol{E}_s^{\text{sp}^H} + \boldsymbol{E}_n^{\text{sp}} \boldsymbol{\Lambda}_n^{\text{sp}} \boldsymbol{E}_n^{\text{sp}^H}$;
6. $\hat{\boldsymbol{r}}_1 = \underset{[0, d^{\text{sp}}_{\text{unamb}}]}{\text{findpeaks}} \frac{1}{\boldsymbol{a}_r^{\text{sp}^H} \boldsymbol{E}_n^{\text{sp}} \boldsymbol{E}_n^{\text{sp}^H} \boldsymbol{a}_r^{\text{sp}}}$;
7. $K = \text{length}(\hat{\boldsymbol{r}}_1), P = \left\lceil \frac{d_{\max}}{d^{\text{sp}}_{\text{unamb}}} \right\rceil$;
8. $\hat{\boldsymbol{r}}_1' = \text{ones}(1, P) \otimes \hat{\boldsymbol{r}}_1 + d^{\text{sp}}_{\text{unamb}}(0{:}P-1) \otimes \text{ones}(1, K)$;
// Stage 2. Ambiguity removal
9. $N_L = \rho N$, $N_{\text{sub}} = N - N_L + 1$;
10. Obtain sparse data matrix after MSSP $\hat{\boldsymbol{Y}}$;
11. $\boldsymbol{R}_{\hat{Y}} = \frac{1}{N_{\text{sub}} M} \hat{\boldsymbol{Y}} \hat{\boldsymbol{Y}}^H$;
12. $\boldsymbol{R}_{\hat{Y}} = \boldsymbol{E}_s \boldsymbol{\Lambda}_s \boldsymbol{E}_s^H + \boldsymbol{E}_n \boldsymbol{\Lambda}_n \boldsymbol{E}_n^H$;
13. $P_{\text{MUSIC}}(\hat{\boldsymbol{r}}_1') = \frac{1}{\boldsymbol{a}_r^H \boldsymbol{E}_n \boldsymbol{E}_n^H \boldsymbol{a}_r}$;
14. Obtain the verified spectral peaks $\hat{\boldsymbol{r}}$;
15. **return** $\hat{\boldsymbol{r}}$.

The two stages of Algorithm 1 can be explained as follows. In the first stage, all possible ranges of targets are found via the MUSIC spectrum of the decimated sparse data and periodic extension. Specifically, in Step 1, the decimated sparse data matrix $\tilde{\boldsymbol{Y}}^{\text{sp}}$ is obtained by uniformly decimating the total collocated OFDM data matrix $\tilde{\boldsymbol{Y}}$ with a step size of η. Then, MSSP is performed on $\tilde{\boldsymbol{Y}}^{\text{sp}}$ in Steps 2–3, and MUSIC is performed in the maximum unambiguous range of decimated sparse data $d^{\text{sp}}_{\text{unamb}} = \frac{c}{2\eta\Delta f}$ to obtain the coarse range estimation $\hat{\boldsymbol{r}}_1$ in Steps 4–6. Subsequently, as shown in Steps 7–8, all possible ranges of targets $\hat{r}_1'$ are obtained by periodic extension of spectral peaks $\hat{r}_1$ searched by MUSIC, where d_{max} denotes the maximum detection range of OFDM radar, $P = \left\lceil \frac{d_{max}}{d_{unamb}^{sp}} \right\rceil$ denotes the number of extended periods, and $\otimes$ denotes the Kronecker product. In the second stage, all possible ranges of targets are verified by the MUSIC spectrum of the collocated subcarrier data individually to remove the range ambiguity. As is shown in Steps 9 – 10, MSSP is performed on $\tilde{Y}$. Then, calculation and eigenvalue decomposition of the connivance matrix are performed in Steps 11 – 12. Finally, all possible ranges in $\hat{r}_1'$ are verified by the MUSIC spectrum of the collocated subcarrier data point-by-point, where the spectral values at the true peaks are large, as is shown in Steps 13 – 14.

The range estimation result of the proposed scheme and traditional MUSIC is shown in Fig. 4. As shown by the black solid line, spectrum search is performed in the maximum unambiguous range for decimated sparse data in the first stage. Then, all possible ranges of targets are obtained by periodic extension, as shown by the red dashed line. Finally, in the second stage, the MUSIC pseudospectrum of the total collocated subcarrier data is used to check each possible range to remove any ambiguity, as shown by the blue solid line. The lower data dimension of decimated sparse data, smaller range for spectrum search, and limited points to be checked by the total collocated subcarrier data make the complexity of the proposed two-stage scheme much lower than that of the traditional MUSIC. In the following part, numerical results are provided to compare the complexity of the proposed scheme and the traditional MUSIC.

4.3 Computational Complexity Analysis

For the MUSIC algorithm, the computational complexity for calculating the covariance matrix is $\mathcal{O}\left(MN^2\right)$, and the complexity of eigenvalue decomposition and spectrum search is $\mathcal{O}\left(N^3\right)$ and $\mathcal{O}\left(\left(2N(N-K)+N\right)r\right)$, respectively. Thus, the complexity of traditional MUSIC after spatial smoothing is $\mathcal{O}\left(N_{sub}MN_L^2 + N_L^3 + \left(2N_L\left(N_L-K\right)+N_L\right)r\right)$, where r denotes the number of points calculated in the peak search. Assuming the proposed scheme is applied to MUSIC, the complexity of the two stages of the proposed scheme is $\mathcal{O}\left(N_{sub}^{sp}MN_L^{sp\,2} + N_L^{sp\,3} + \left(2N_L^{sp}\left(N_L^{sp}-K\right)+N_L^{sp}\right)r'\right)$ and $\mathcal{O}\left(N_{sub}MN_L^2 + N_L^3 + \left(2N_L\left(N_L-K\right)+N_L\right)KP\right)$.

Assume the number of total collocated subcarriers is $N = 1\,024$, the number of OFDM symbols is $M = 112$, the maximum detection range of OFDM radar is $d_{max} = 300$ m, the step size for spectrum search is 0.01 m, and the number of targets is $K = 3$. Then a comparison of the complexity of traditional MUSIC, PM-MUSIC and the proposed scheme with different decimation intervals η is provided in Table 1. It is observed that the PM-MUSIC algorithm can only slightly reduce the computational complexity of the MUSIC algorithm. The proposed scheme, however, can not only significantly reduce the complexity of MUSIC, but also further reduce the complexity of PM-MUSIC.

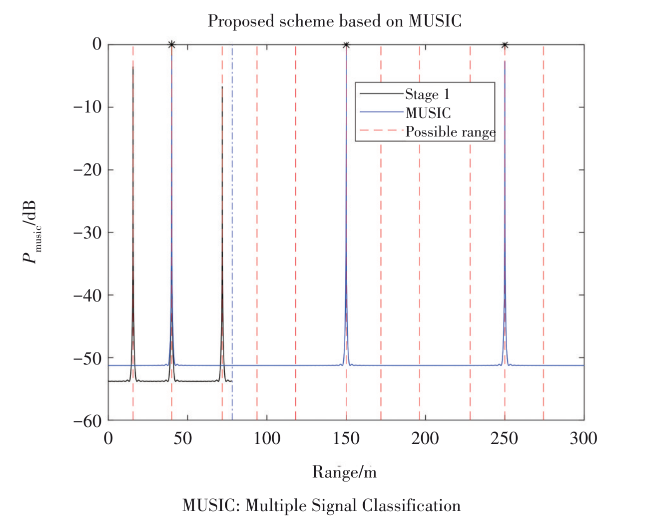

▲ **Figure 4. Range estimation result of the proposed scheme and traditional MUSIC**

5 Simulation Results

In this section, the performance of the two-stage algorithms is verified. The relevant parameter settings are as follows. The subcarrier spacing is $\Delta f = 120$ kHz, the total number of subcarriers is $N = 1\,024$, and thus the total bandwidth is $B = 122.88$ MHz. Moreover, the number of OFDM symbols is $M = 112$, the maximum detection range of OFDM radar is $d_{max} = 300$ m, and the number of targets is $K = 3$.

As is shown in Fig. 5(a), a comparison of MUSIC, PM-MUSIC, and the proposed scheme in terms of root mean square error (RMSE) of the range estimations is provided. It is observed that the RMSEs of the proposed scheme are at the centimeter level, that is, the proposed algorithms can achieve comparable range estimation accuracy with traditional MUSIC and PM-MUSIC. In Fig. 5(b), the RMSEs of Algorithm 1 with different decimation intervals η are provided. It is observed that at low SNR levels, the estimation accuracy

▼**Table 1. Computational complexity analysis**

Algorithms	Complexity of Different Decimation Intervals		
	$\eta = 8$	$\eta = 16$	$\eta = 32$
MUSIC		1.59e10	
Proposed+MUSIC	3.80e8	2.73e8	2.65e8
PM-MUSIC		1.57e10	
Proposed+PM-MUSIC	2.46e8	1.40e8	1.32e8

MUSIC: Multiple Signal Classification PM: Propagator Method

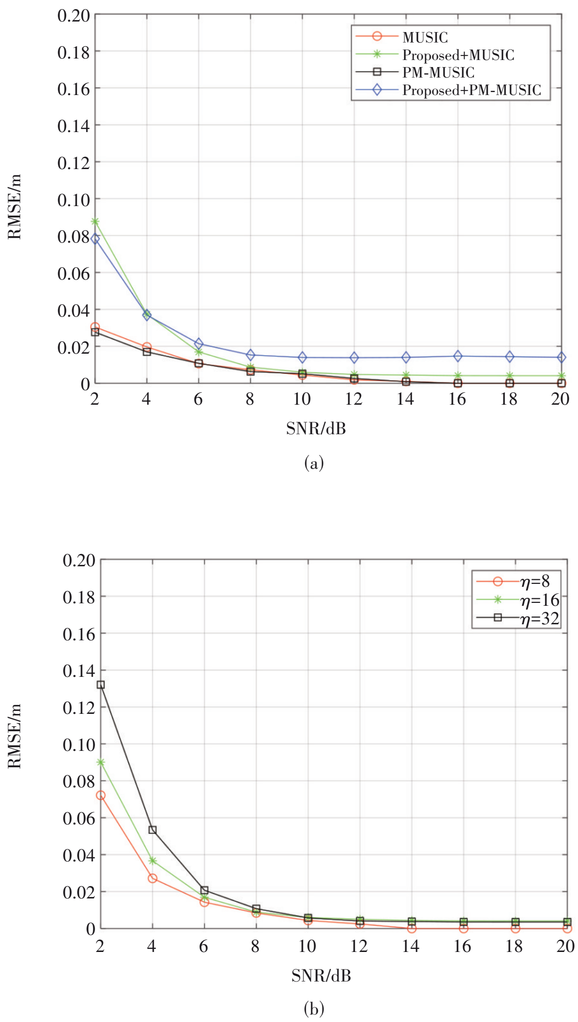

RMSE: root mean square error MUSIC: Multiple Signal Classification
PM: Propagator Method

▲ Figure 5. (a) RMSE of MUSIC, PM-MUSIC, and the proposed scheme for range estimation; (b) RMSE of the proposed scheme with different decimation intervals for range estimation

of the proposed scheme slightly decreases as the decimation interval increases.

6 Conclusions

In this paper, we reduce the computational complexity of range estimation by uniformly decimating in the subcarrier domain, and derive the mathematical relationship between range resolution, maximum unambiguous range and the decimation interval. Then, a two-stage scheme is proposed to achieve low-complexity high-resolution range estimation while maintaining the unambiguous range, which first exploits the low-dimension data matrix to reduce computational complexity, and then removes the range ambiguity utilizing total collocated subcarrier data. Finally, we compare the complexity and performance of the proposed scheme with traditional MUSIC and PM-MUSIC, and the results show that the proposed two-stage scheme can significantly reduce the complexity of range estimation with minimal performance degradation. Besides, the proposed scheme can be easily adapted to super-resolution algorithms for Doppler and AoA estimation.

References

[1] ITU. Framework and overall objectives of the future development of IMT for 2030 and beyond [R]. 2023

[2] SIT Y L, STURM C, REICHARDT L, et al. The OFDM joint radar-communication system: an overview [C]//Proceedings of the International Conference Advances in Satellite and Space Communications. IEEE, 2011: 69 – 74

[3] ZHANG C Y, ZHOU Z W, WANG H Z, et al. Integrated super-resolution sensing and communication with 5G NR waveform: Signal processing with uneven CPs and experiments: (invited paper) [C]//The 21st International Symposium on Modeling and Optimization in Mobile, Ad Hoc, and Wireless Networks (WiOpt). IEEE, 2023: 681 – 688. DOI: 10.23919/wiopt58741.2023.10349843

[4] XIAO Z Q, ZENG Y. Waveform design and performance analysis for full-duplex integrated sensing and communication [J]. IEEE journal on selected areas in communications, 2022, 40(6): 1823 – 1837. DOI: 10.1109/JSAC.2022.3155509

[5] CUI Y H, LIU F, JING X J, et al. Integrating sensing and communications for ubiquitous IoT: applications, trends, and challenges [J]. IEEE network, 2021, 35(5): 158 – 167. DOI: 10.1109/MNET.010.2100152

[6] CHENG X, DUAN D L, GAO S J, et al. Integrated sensing and communications (ISAC) for vehicular communication networks (VCN) [J]. IEEE Internet of Things journal, 2022, 9(23): 23441 – 23451. DOI: 10.1109/JIOT.2022.3191386

[7] BRAUN M. OFDM Radar algorithms in mobile communication networks [D]. Karlsruhe: Karlsruher Instituts für Technologie (KIT), 2014

[8] SCHMIDT R. Multiple emitter location and signal parameter estimation [J]. IEEE transactions on antennas and propagation, 1986, 34(3): 276 – 280. DOI: 10.1109/TAP.1986.1143830

[9] ROY R, KAILATH T. ESPRIT-estimation of signal parameters via rotational invariance techniques [J]. IEEE transactions on acoustics, speech, and signal processing, 1989, 37(7): 984 – 995. DOI: 10.1109/29.32276

[10] RAO B D, HARI K V S. Performance analysis of Root-Music [J]. IEEE transactions on acoustics, speech, and signal processing, 1989, 37(12): 1939 – 1949. DOI: 10.1109/29.45540

[11] PESAVENTO M, GERSHMAN A B, HAARDT M. Unitary root-MUSIC with a real-valued eigen decomposition: a theoretical and experimental performance study [J]. IEEE transactions on signal processing, 2000, 48 (5): 1306 – 1314. DOI: 10.1109/78.839978

[12] MARCOS S, MARSAL A, BENIDIR M. Performances analysis of the propagator method for source bearing estimation [C]//International Conference on Acoustics, Speech and Signal Processing. IEEE, 1994: IV/237 – IV/240. DOI: 10.1109/ICASSP.1994.389823

[13] TAYEM N, KWON H M. L-shape 2-dimensional arrival angle estimation with propagator method [J]. IEEE transactions on antennas and propagation, 2005, 53(5): 1622 – 1630. DOI: 10.1109/TAP.2005.846804

[14] NI Z T, ZHANG J A, HUANG X J, et al. Uplink sensing in perceptive mobile networks with asynchronous transceivers [J]. IEEE transactions on signal processing, 2021, 69: 1287 – 1300. DOI: 10.1109/TSP.2021.3057499

[15] CHEN L L, QI W D, LIU P, et al. Low-complexity joint 2-D DOA and

TOA estimation for multipath OFDM signals [J]. IEEE signal processing letters, 2019, 26(11): 1583 – 1587. DOI: 10.1109/LSP.2019.2936292

[16] YAMADA H, OHMIYA M, OGAWA Y, et al. Super-resolution techniques for time-domain measurements with a network analyzer [J]. IEEE transactions on antennas and propagation, 1991, 39(2): 177 – 183. DOI: 10.1109/8.68179

Biographies

DAI Qianglong received his BS degree in electronic and information engineering from Nanjing University of Posts and Telecommunications, China in 2023. He is currently pursuing his MS degree with the National Mobile Communications Research Laboratory, Southeast University, China. His research interests include ISAC and OFDM.

ZHOU Zhiwen received his BS degree in electronic and information engineering from Nanjing University of Posts and Telecommunications, China in 2022. He is currently pursuing his MS degree with the National Mobile Communications Research Laboratory, Southeast University, China. His research interests include ISAC and XL-arrays.

XIAO Zhiqiang received his BS and MS degrees from Nanjing University of Posts and Telecommunications, China in 2017 and 2020, respectively. He is currently pursuing his PhD degree with the National Mobile Communication Research Laboratory, Southeast University, China, and Purple Mountain Laboratories. His research interests include ISAC, waveform design and optimization, massive MIMO communications, and wireless localization.

ZENG Yong (yong_zeng@seu.edu.cn) is a full professor with the National Mobile Communications Research Laboratory, Southeast University, China, and also with the Purple Mountain Laboratories. He received both the BE (First-Class Honours) and PhD degrees from Nanyang Technological University, Singapore. From 2013 to 2018, he was a research fellow and senior research fellow at the Department of Electrical and Computer Engineering, National University of Singapore. From 2018 to 2019, he was a lecturer at the School of Electrical and Information Engineering, the University of Sydney, Australia. Dr. ZENG was a highly cited researcher by Clarivate Analytics for five consecutive years (2019 – 2023). He is the recipient of the Australia Research Council (ARC) Discovery Early Career Researcher Award (DECRA), 2020 and 2024 IEEE Marconi Prize Paper Awards in Wireless Communications, 2018 IEEE Communications Society Asia-Pacific Outstanding Young Researcher Award, 2020 and 2017 IEEE Communications Society Heinrich Hertz Prize Paper Awards, 2021 IEEE ICC Best Paper Award, and 2021 China Communications Best Paper Award. He has published more than 170 papers, which have been cited by more than 26 000 times based on Google Scholar.

YANG Fei received his BS and PhD degrees in communication and information system in 2009 and 2014, respectively, both from University of Science and Technology of China (USTC). He joined Huawei Technologies Co., Ltd. since 2014. He has worked in departments of radio access network (RAN) chipset algorithm R&D and cell-phone communication protocol and technology. He is now a principal engineer in Wireless Technology Laboratory. His research interests include 6G channel modeling and integrated communication and sensing (ISAC) and their RAN simulation methodologies.

CHEN Yan is a senior expert of wireless communication at Huawei Technologies Co., Ltd. She received her BS and PhD degrees from Chu Kochen Honored College and Institute of Information and Communication Engineering, Zhejiang University, China in 2004 and 2009, respectively. Her research interests include 6G vision and enabling technology study (e.g., use cases, key capabilities, evaluation methodologies, and emerging technologies such as ISAC and collaborative robotics enabled by integrated sensing, artificial intelligence, and communications).